



# Predicting the remaining service life of land concrete by steel corrosion

Woo-Yong Jung<sup>a</sup>, Young-Soo Yoon<sup>b,\*</sup>, Young-Moo Sohn<sup>c</sup>

<sup>a</sup>Structural Division, DongIl Engineering Consultants Corporation, Seoul, South Korea

<sup>b</sup>Department of Civil and Environmental Engineering, Korea University, 5-1 Ga, Anam-Dong Sungbuk-Gu, Seoul, South Korea

<sup>c</sup>Structural Department, Kumho Engineering Corporation, Seoul, South Korea

Received 24 September 2001; accepted 22 October 2002

## Abstract

This paper presents the prediction of remaining service life of the land concrete as distinguished from the marine concrete. This study assumes that the land concrete is deteriorated by following three cases: carbonation, using sea sand and using deicing salts. In case of carbonation deterioration, statistical analysis and the depth of carbonation front are considered. This depth is assessed about 3.6–8.3 mm and can give more exact prediction than just carbonation depth by phenolphthalein. In case of using sea sand, various specimens considering chloride contents, carbonation accelerating, cover depth, relative humidity and water cement ratio are measured by linear polarization resistance method and half-cell potential method during the 1 year. And measurements of the real steel loss give the conversion ratio of polarization resistance and corrosion rate; consequently, their results make the prediction equation of rust growth during any specified period. In case of using deicing salts, surface chloride contents that change with time are focused. The proposed methods are considered to be useful for prediction of remaining service life of the land concrete by steel corrosion.

© 2002 Elsevier Science Ltd. All rights reserved.

**Keywords:** Durability; Corrosion; Humidity; Chloride; Carbonation

## 1. Introduction

Researches on the steel corrosion and concrete durability have recently been conducted and attract a lot of attention. Most of these, however, concentrate on the marine concrete and relatively handle less the land concrete. The prediction of service life of the marine concrete, therefore, has got a considerable development [1–3], whereas much efforts to be desired for the land concrete. Furthermore, many studies focus on the relative resistance of concrete rather than the quantitative assessment [4–6]. Although these contributions are significant and helpful to assess the service life, they cannot predict the service life quantitatively. The following causes explain why the predicting service life of land concrete does not develop enough yet. First, the service life of the land concrete, as opposed to the marine concrete, has a less dominant and more complex rate controlling process; thus, it makes much more difficulty to predict specifically and precisely. Secondly, the corrosion of the land concrete is usually being regarded as less severe than that of the marine one. As particularly in Korea, the prediction of service life

of land concrete is, however, called for a more significant since some concretes on land might be mixed in using sea sand with the possibility of imperfect chloride elimination.

For the purpose of predicting service life of land concrete by steel corrosion, this paper assumes that the land concrete is deteriorated by following three cases: carbonation, using sea sand and using deicing salts. The prediction by carbonation deterioration focuses on the statistical analysis and the depth of carbonation front through the investigation of five bridges in Korea. And in case of using sea sand, the corrosion ratio of linear polarization resistance and corrosion rate is assessed by measuring steel loss. Also, the various specimens considering chloride contents, carbonation accelerating, cover depth, relative humidity and water cement ratio are measured by linear polarization resistance method and half-cell potential method during 1 year. And the last case of using deicing salts focus the surface chloride contents that change with time on the basis of previous literature [2].

## 2. Time history of steel corrosion

A steel corrosion progress according to the time has various aspects in correspondence to the conditions specified.

\* Corresponding author. Tel.: +82-2-3290-3320; fax: +82-2-928-7656.  
E-mail address: ysyoon@korea.ac.kr (Y.-S. Yoon).

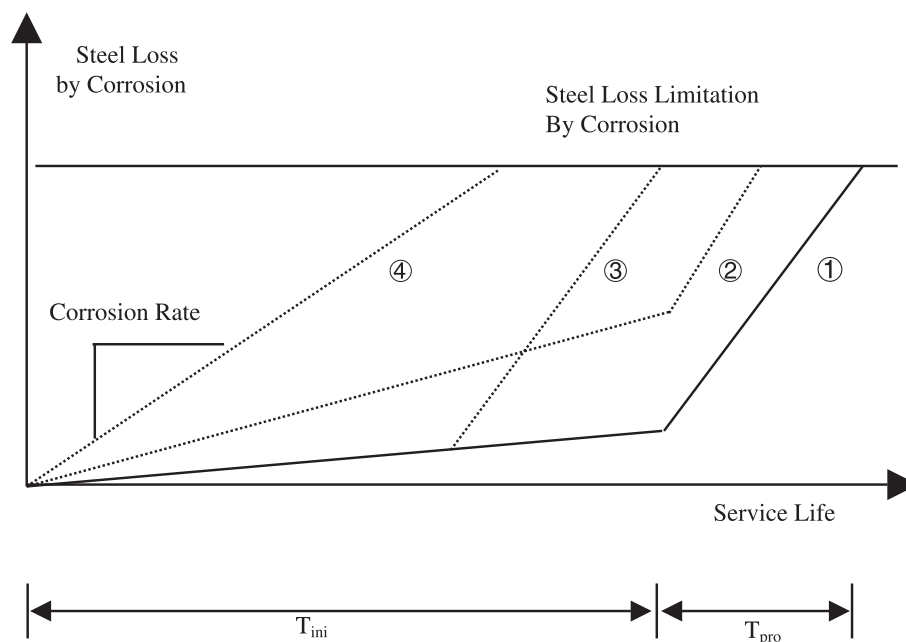


Fig. 1. Steel corrosion according to time.

Transportation of an exterior substance infiltration and reaction such as chloride ion penetration or carbonation induced corrosion progress in curve ① in Fig. 1 but if concrete cover reduced or crack developed, the initiation period  $T_{ini}$  would be mostly shortened as in curve ③ in Fig. 1 [7]. Also, if the concrete include sea sand, the curve shape would change from ① to ② or ④. This paper regards service life as initial period, because propagation period is relatively short. Weyers [1] suggests that the time-to-cracking period is relatively short time period of 3–7 years of the structure service life in chloride-laden environments. Tuutti [20] also presents that, at 10 °C, the propagation period for reinforced concrete structures has been estimated to be 5–10 years for corrosion caused by chlorides. And corrosion of curve ④ such as using sea sand is ambiguous to distinguish initiation period from propagation period.

### 3. Initiation period by carbonation

#### 3.1. Investigation of pH distribution according to concrete depth

Concrete carbonation depth can usually be measured by the phenolphthalein, which indicates from 8.3 to 9.5

pH. However, the corrosion occurs at the range of pH 11–11.5 and the pH threshold for corrosion be raised if chloride ion contents are higher. Therefore, by using four indicators shown in Table 1, the pH distribution assessment has been conducted over five bridges located in Korea as shown in Table 2. The assessment shows that the depth of corrosion threshold is 3.6–8.3 mm deeper than depth by phenolphthalein. Also, this result is similar with 5–10 mm by Broomfield [8] and this more value is called depth of carbonation front. Although this gap can be seemed trivial, this could predict service life differently by 10 years, because the service life is proportional to the square of carbonation depth. And this explains well that sometimes the carbonation depth by phenolphthalein would be measured zero about bridges under the 10 years old.

#### 3.2. pH values of corrosion threshold and effective carbonation depths

The carbonation depth determined by phenolphthalein is different from corrosion threshold depth; therefore, it must

Table 1  
pH range by measurement of various indicator

Indicator	pH range
Tropaeolin O	pH 11.1–12.7
Alizarin yellow R	pH 10.2–12.2
Thymolphthalein	pH 9.3–10.5
Phenolphthalein	pH 8.3–9.5

Table 2  
Investigation of field bridges

Name of bridges	Location	The time of completion
Sum-Gang	Young-Dong highway 60.7 km (Korea)	1971
Ja-San	Young-Dong highway 60.6 km (Korea)	1971
Dong-Hoa	Young-Dong highway 78.3 km (Korea)	1971
Sok-Sa-Chon	Young-Dong highway 151.2 km (Korea)	1975
Kim-Chon	Kyung-Bu highway 229.4 km (Korea)	1970

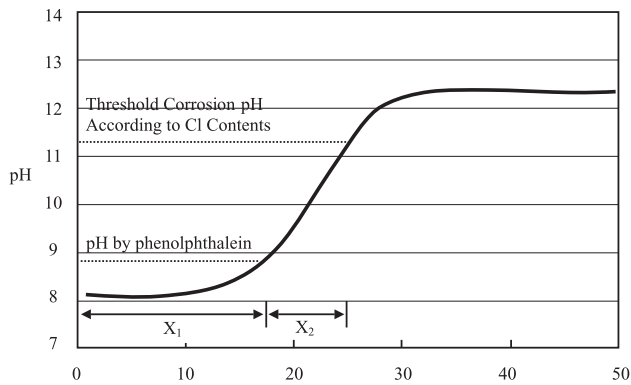


Fig. 2. Threshold corrosion pH according to Cl contents.

be modified as in Fig. 2 and effective cover depth is expressed as Eq. (1).

$$x = x_1 + x_2 \quad (1)$$

where  $x$  is effective carbonation depth,  $x_1$  is the carbonation depth by phenolphthalein and  $x_2$  is the depth of carbonation front that is varied as chloride ion contents, but ordinarily it can be assumed 6 mm, which is the average of 3.6 and 8.3 by Table 3, in the case of little chloride contents concrete.

### 3.3. Statistical assessment of effective cover depths and corrosion limits

Concrete cover gives protection against the exterior infiltration in the form of a fluid or gas; therefore, deeper concrete depth usually makes a better resistance against chloride ion and carbonation. Concrete cover depth can not be considered as the constant value but be statistically assessed considering reduction of the real cover depth by surface cracks and nonuniform placement of embedded steel by the normal distribution. This paper considers only the dispersion tendency of a steel embedment during construction because the effect and distribution of cracks are difficult to be considered at current level.  $\alpha$  is standard normal probability parameter in Table 4, which means maximum

Table 4

Steel loss limit and standard normal probability parameter ( $\alpha$ )

Loss limit by corrosion (%)	Standard normal probability parameter ( $\alpha$ )
1	2.33
2.5	1.96
5.0	1.65
10	1.28
20	0.85
30	0.52

limitation of allowable corroded reinforcement. In the deck of bridge, the  $\sigma$  value is investigated by Weyers [9] as 8 mm in 50-mm concrete cover.

$$d = d_1 - \alpha\sigma \quad (2)$$

Where  $d$  and  $d_1$  are the effective cover depth and the design cover depth, respectively. Also,  $\alpha$  and  $\sigma$  are the normal probability parameter and the standard deviation of a cover depth, respectively.

### 3.4. Effect of relative humidity about carbonation

The relation between carbonation and time can be expressed as Eq. (3) in which  $n$  may be determined by relative humidity as suggested by Parrott [8,10]. Otherwise, 0.5 can be used as a default value. The constant  $k$  changes according to the kinds of cements, w/c, relative humidity and so on; therefore, it is recommended to be induced from the ages and carbonation depth by field investigation rather than using the various recommending equations at by previous literatures.

$$x = kT_{\text{ini}}^n \quad (3)$$

$$n = 0.02536 + 0.01785r - 0.0001623r^2 \quad (4)$$

where  $r$  is relative humidity but  $n$  is 0.5 if  $r$  is less than 60% [8].

Table 3

Carbonation depth by various indicators (mm)

Investigated place		Phenolphthalein	Thymolphthalein	Alizarin	Tropaeolin
Sum-Gang	Pier	3.7	6.6	7.5	12.3
	Abut	14.5	15.0	17.6	19.9
	Abut	13.3	15.7	19.8	21.4
Ja-San	Abut	28.6	32.5	35.7	39.2
	Abut	12.1	18.9	19.4	23.1
Dong-Hoa	Abut	5.8	8.0	10.5	11.0
	Abut	5.1	6.0	8.6	8.3
Sok-Sa-Chon	Abut	6.3	9.7	13.4	15.9
Kim-Chon	Slab	16.4	19.1	21.7	22.6
	Slab	9.3	19.3	22.8	24.1
Average		11.5	15.1	17.7	19.8
Different depth by phenolphthalein		0	3.6	6.2	8.3

#### 4. Quantitative evaluation of steel corrosion

##### 4.1. Test description

The quantitative test of steel corrosion was carried out like as Fig. 3 depicts the whole sequence of the test. Based on ASTM G59-91 [11], linear polarization resistance was determined by measuring the change of current during sweeping potential from  $-30$  to  $+30$  mV at a rate  $0.167$  mV/s using Potentiostat M273 from EG&G. The linear polarization resistance is expressed as corrosion rate using conversion coefficient ( $B$ ), which is experimentally determined by comparing measured steel loss with integration of the reciprocal of polarization resistance with respect to time. In carbonation condition, the carbonating of specimens was accelerated until carbonation depth by phenolphthalein is deeper than 20 mm in conditions of  $\text{CO}_2$  10%, temperature  $20 \pm 2$  °C, humidity  $50 \pm 5\%$ . And corrosion rates in humidity condition were expressed as an equation of multiple regression analysis by the SAS program. The mass difference between primary steel before placement and corroded steel was measured by sand brush to 1/100 g accuracy and oxidized film mass is considered by measuring many another oxidized film mass. In addition to the qualitative test that is generally used, half-cell potential method based on ASTM C876 [12] was carried out and compared with the polariza-

tion resistance test. Fig. 4 shows the polarization resistance experiment device. The counter and reference electrode were embedded in concrete because exterior electrode could transport chloride ions in electrolyte into inner concrete. Stainless was used as a reference electrode ( $R$ ) and carbon as a counter electrode. The deformed bar corresponding to working electrode ( $W$ ) has 10-mm diameter, 200-mm length and  $58.5\text{-cm}^2$  surface area. The size of specimen is  $25 \times 20 \times 10$  cm and every surface except upper surface was coated with paraffin. The exposed portions of steel were coated with silicon without acetic acid. The specimens have three different cover depths of 20, 30 and 40 mm. Table 5 shows concrete mixture properties and 101 bars were measured over 500 times. The specimens have the following designation as  $\circ \diamond \square - \triangle$  and each  $\circ$ ,  $\diamond$ ,  $\square$  and  $\triangle$  stands for w/c, surrounding conditions, the chloride ion contents and concrete cover, respectively. For example, 50C0.2–30 represents that w/c is 50%; surrounding condition is carbonation acceleration; chloride ion contents by cement weight is 0.2% and pure concrete cover depth 20 mm.

##### 4.2. Relationship between polarization resistance and corrosion rate

To measure the corrosion rate there are methods such as linear polarization resistance method, the AC impedance

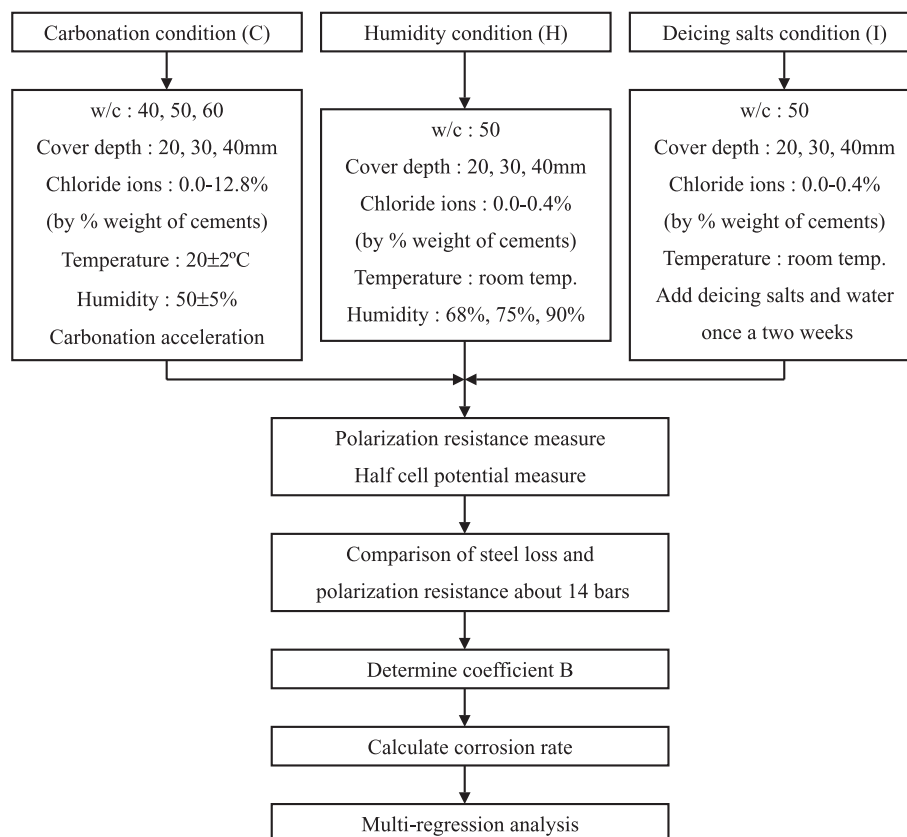


Fig. 3. Experiment flow chart.

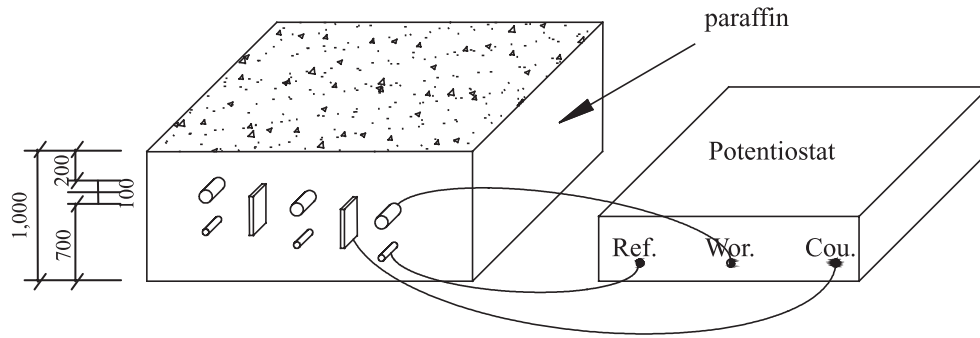


Fig. 4. Polarization resistance experiment device.

method, electrochemical noise method and Taffel method. But the AC impedance method and electrochemical noise method have rather complicated application and the inconvenience to be used in the field. In the case of Taffel method, it takes a long time and induces the corrosion during the test [13,14]. On the other hand, linear polarization resistance method is simple to be applied and there is no induction of corrosion during the test. But the Taffel coefficient is necessary to apply polarization resistance method exactly,  $\beta_a$  and  $\beta_c$  as indicated in Eq. (5).

However, these coefficients are not determined without using the Taffel method and they are difficult to be determined exactly in concrete [15]. To overcome these problems, the test was performed to analogize the conversion coefficient  $B$  comparing the steel loss to the value that integrates the inverse number of polarization with respect to the time because the corrosion current can be converted into the mass by Eq. (6) of the Faraday's law. And comparison is conducted about 11 bars, which are relatively much corroded for 1 year. In fact, the  $B$  value varies according to time and concrete condition. But Fig. 5 shows that  $B$  is not much variable and determination of each value about each case demands so much works, thus this paper assumed  $B$  as constant. Although the potential drop of the resistance to the concrete must be considered as well to determine  $R_p$ , it does not matter because the  $B$  value itself is the result considering potential drop.

$$R_p = \frac{dV}{di_{app}} = \frac{\beta_a \beta_c}{2.3 i_{corr} (\beta_a + \beta_c)} = \frac{B}{i_{corr}} \quad (5)$$

$$m = \frac{Mi_{corr}t}{zF} \quad (6)$$

$$Q_{corr} = \frac{55.85 \times A}{2 \times F} \int di_{corr} dt = \frac{55.85 \times A \times B}{2 \times 96,500} \int \frac{dt}{dR_p} \quad (7)$$

Here,  $R_p$ : the polarizing resistance ( $\Omega \cdot \text{cm}^2$ ),  $V$ : voltage (V),  $B$ : conversion coefficient,  $m$ : a mass (g),  $\beta_a$ : anodic Taffel coefficient,  $\beta_c$ : cathodic Taffel coefficient,  $i_{corr}$ : a corrosion current ( $\text{A}/\text{cm}^2$ ),  $A$ : a steel area ( $\text{cm}^2$ ),  $t$ : specific period,  $M$ : one molecular mass (55.85 g) of the steel,  $z$ : the number of ions and  $Q_{corr}$ : corrosion mass (g). Here, the  $z$  value is 2; the  $F$  is 96,500 A.

#### 4.3. Characteristic of corrosion under various conditions

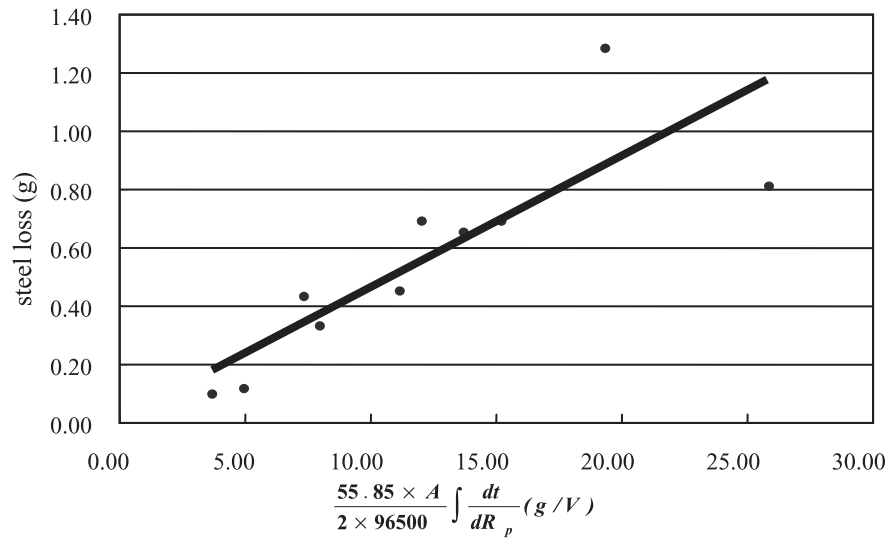
##### 4.3.1. Characteristic of corrosion by chloride ion contents

The threshold chloride ion contents are related with the pH and the a little drop of the pH near the reinforcement steel can develop corrosion even with a small chloride ion contents. Furthermore, the concrete that has much chloride ions can develop corrosion initially regardless of pH. When sea sand is used, the most problematic is that corrosion can generate from an early age in the case that the contained chloride ion contents exceed threshold chloride ion contents. This means that corrosion continues still even if the concrete cover depth is increased.

Figs. 6 and 7 show the polarization resistance and the half-cell potential to the age according to the chloride ion contents. The polarization resistance that represents the quantitative corrosion rate shows some definite inclination according to chloride ion contents, but the half-cell potential shows just whether the corrosion develops qualitatively or not and does not show definite inclination at the early stage. Fig. 8 shows that corrosion rate is unstable up to 100 days. And then it has a definite inclination according to the chloride ion contents. It is so because the hydration reaction of the concrete is not completed yet at the early age and lots of inner water remains. Hence, it is appropriate to measure

Table 5  
Concrete mixture proportions

w/c	C (kg/m <sup>3</sup> )	W (kg/m <sup>3</sup> )	S (kg/m <sup>3</sup> )	G (kg/m <sup>3</sup> )
0.4	445	180	719	1024
0.5	348	180	731	1068
0.6	297	180	774	1097

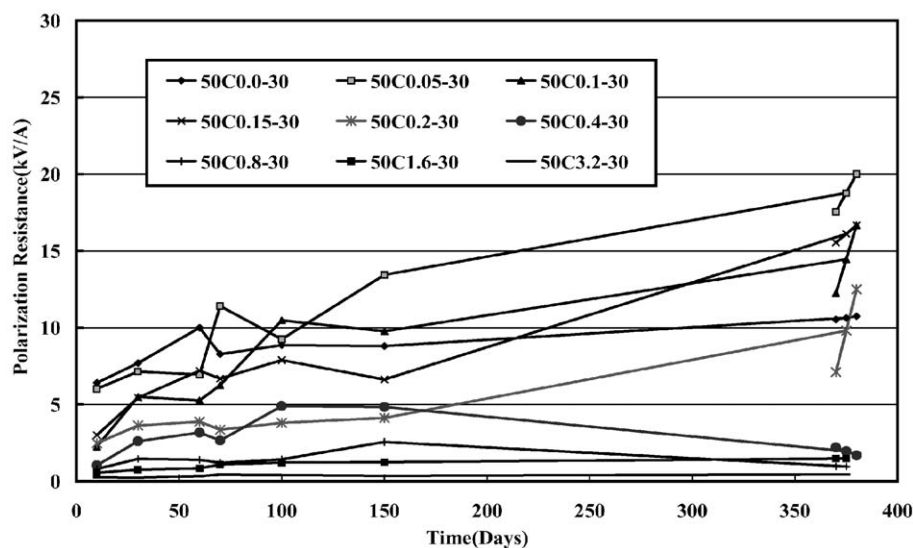
Fig. 5. Regression for determining coefficient  $B$ .

the corrosion rate after 100–150 days and this agrees with the existing researches [16].

#### 4.3.2. Characteristic of corrosion according to relative humidity

The corrosion by carbonation or chloride ion needs moisture. In general, little corrosion occurs when the relative humidity is under 60% with no chloride ion. And the corrosion rate increases if relative humidity increases and decreases if relative humidity is over some value [10]. Also the corrosion may be developed under the 60% if the chloride ion contents are sufficient. The characteristic of the corrosion was, herein, measured in three different humidity conditions at room temperature.

Four measurements was carried out at a 90-day-interval for 360 days. Till 90 days, the specimens were kept indoor at the identical conditions and after 90 days they were categorized into the three cases; one case is under condition of no water sprinkled, no plastic wrapping (average 68%, HA), another case is under condition of a little water sprinkled, wrapped with plastic (average 75%, HB), the other case is under the condition of a lot of water sprinkled, wrapped with plastic (average 90%, HC). The corrosion rate and the half-cell potential according to the relative humidity are shown in Figs. 9 and 10. As the relative humidity increases, the corrosion rate increases and as the chloride ion contents increases, the inclination of corrosion rate according to the relative humidity be-

Fig. 6. Polarization according to time and chloride ion for  $w/c=0.5$ , cover depth 30 mm.



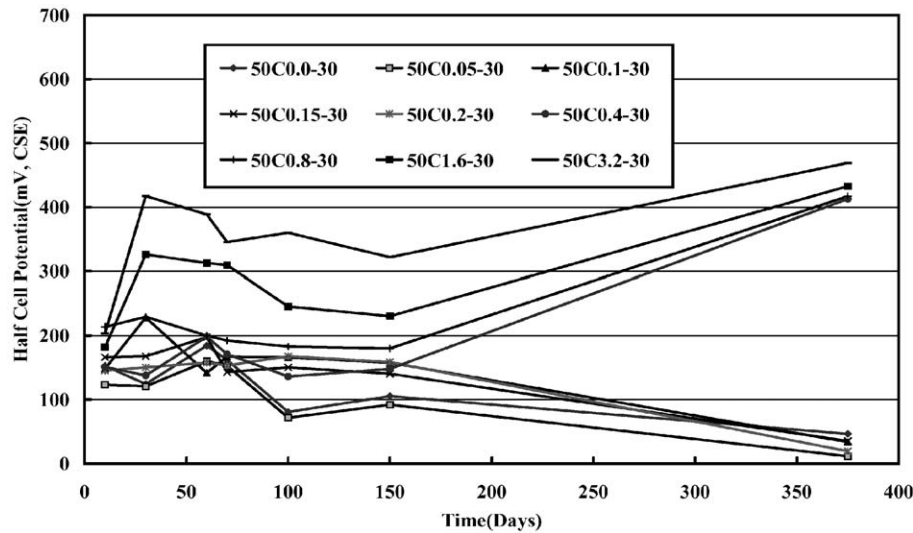


Fig. 7. Half-cell potential according to time and chloride ion for  $w/c = 0.5$ , cover depth 30 mm.

comes higher. The half-cell potential also shows similar inclination.

#### 4.3.3. Characteristic of corrosion according to concrete cover depth

As the concrete cover becomes thicker, the effect of the external infiltrator substance such as water, chloride ion, deicing salts and carbonation is decreased. Also the damage of cracks would be reduced. However, concrete using sea sands can develop corrosion regardless of the cover depth. Moreover, inner part of concrete have more water than outer part if it is in a dry environment for a long time after raining [7]. In Fig. 11, as the cover depth increases, the corrosion rate decreases but inclination of decrement is a relatively

little negative because damage of inserted chlorides is not much affected by cover depth. And Fig. 12 does not show any clear inclination of the half-cell potential according to the concrete cover.

#### 4.3.4. Characteristic of corrosion according to $w/c$ ratio

If the  $w/c$  is higher, the void ratio becomes higher and the interior humidity increases more rapidly. Therefore, the concrete also contains a lot of water contents when the humidity rises. Conversely, the low humidity makes a rapid drop of the interior humidity [17]. So  $w/c$  ratio in relation with humidity effect corrosion rate. The average corrosion rate and the half-cell potential to the  $w/c$  value of the standard specimens are represented in Figs. 13 and

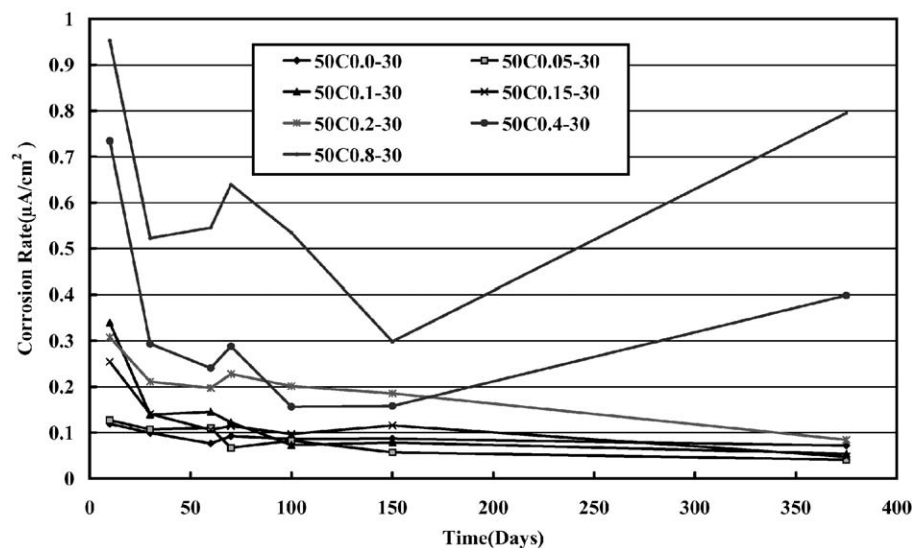


Fig. 8. Corrosion rate according to time and chloride ion for  $w/c = 0.5$ , cover depth 30 mm.

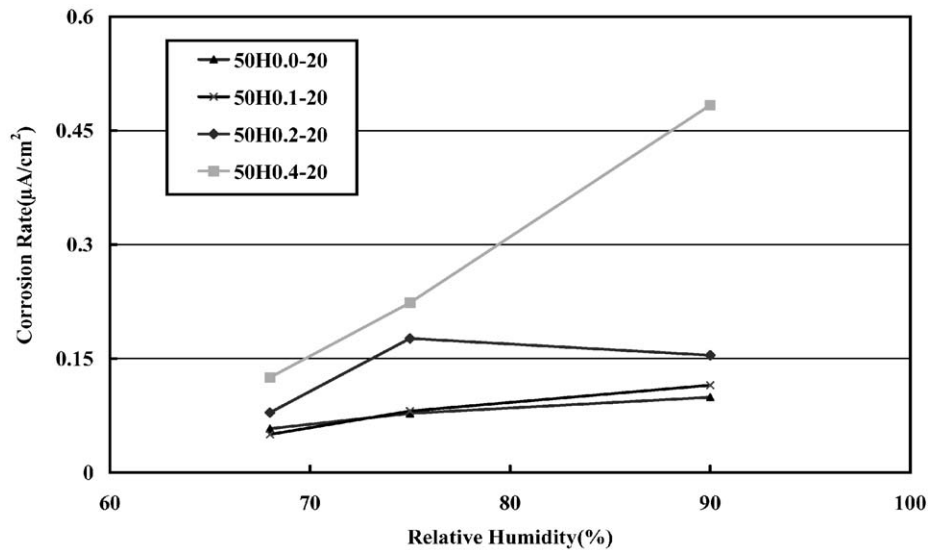


Fig. 9. Corrosion rate according to humidity for  $w/c=0.5$ , cover depth 20 mm.

14 and both do not show any definite inclination. This shows that low humidity (here is 50%) is unable to reflect the characteristic of the void ratios to the corrosion.

#### 4.3.5. Characteristic of corrosion according to carbonation

Carbonation is an inevitable process as long as the concrete is exposed to the air. But the service life of the concrete that has thicker cover depth is not much affected by the carbonation because the carbonating operation generally shows slow proceeding. But when the cover depth is insufficient or the deterioration reason is not distinct, carbonation can be the deterioration rate-controlling factor. Generally, it is difficult for  $CO_2$  to infiltrate in the moisture-saturated condition and to react with the concrete in the dry

condition. Parrott reports that the process of the carbonation is most active in the relative humidity condition from 50% to 60%. It is known that the corrosion owing to the carbonation is fastest in the relative humidity condition from 95% to 98% because the oxygen and water feed rate acts as an important factor [10]. Also, in the relative humidity condition under 60%, there is little corrosion even if carbonation may generate [10]. Fig. 15 shows the measured data from the beginning to the state that the carbonation progressed to 20–25 mm. But the corrosion rate decreased, except for the chloride ion contents 0.4, after the concrete carbonation. This shows little corrosion under the relative humidity condition of 50% even if carbonation may occur, and the half-cell potential also shows the similar results as depicted in Fig. 16.

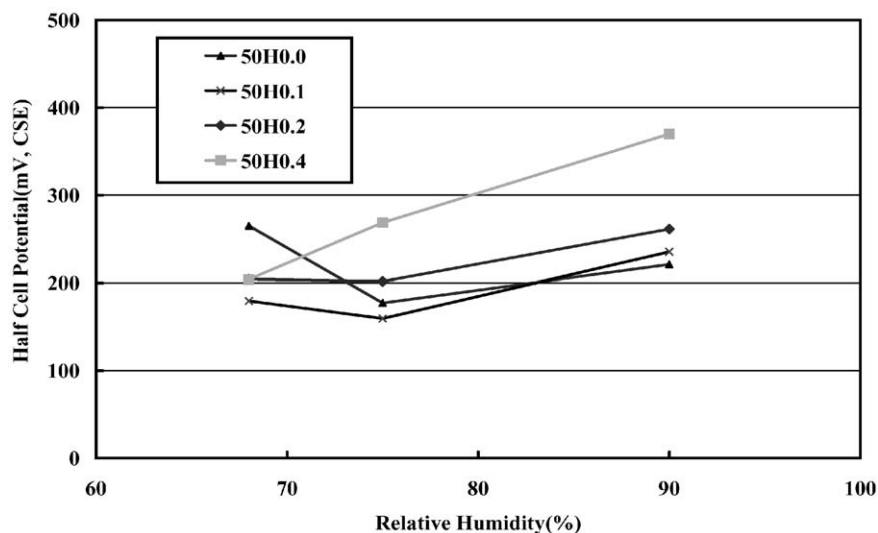


Fig. 10. Half-cell potential according to humidity  $w/c=0.5$ , cover depth 20 mm.



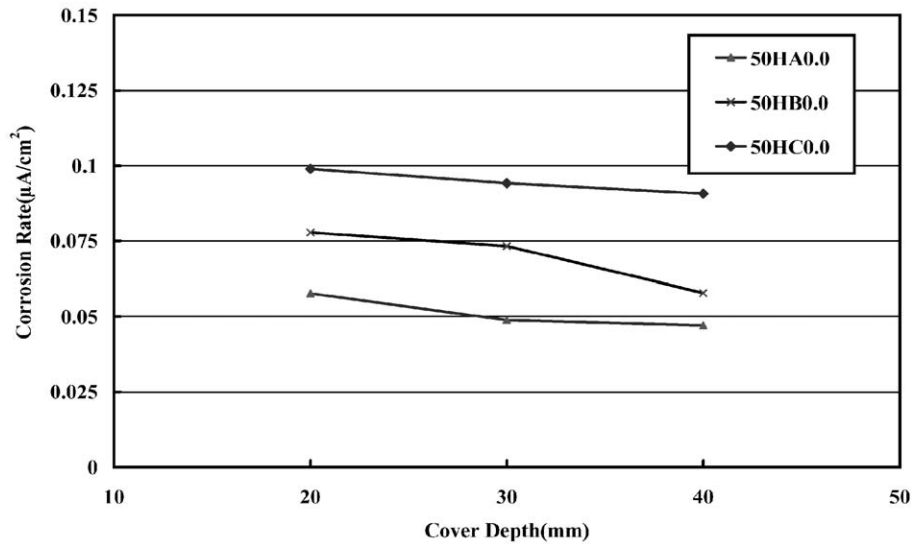


Fig. 11. Corrosion rate according to cover depth for  $w/c=0.5$ ,  $cl0.0$ .

#### 4.3.6. Characteristic of corrosion according to deicing salts

The usage of the deicing salts gives serious corrosion damages on the top deck of concrete bridges on land. The deicing salts are transported into the inside of the concrete by the diffusion and the penetration and can cause the serious harm to concrete when crack progresses to the steel. It is very important how much and how often to use the deicing salts but there is no standard code to set the amount and the frequency. Therefore, it must be decided case by case through field investigation of each bridge. In this paper the value of corrosion rate was measured under the hermetically sealed condition at a 90-day-interval for 360 days and the deicing salts and a water was added once a 2 weeks after 90 day ages. As in Figs. 17 and 18, the use of the deicing salts takes a sudden turn in the corrosion rate and the half-cell potential. The corrosion rate considerably increased in

case of a 20-mm cover depth but there was little clear difference in the case of 30 and 40 mm.

### 5. Prediction method of service life of land concrete by steel corrosion

The prediction of remaining service life of the land concrete by steel corrosion was conducted in three different cases as follows. It is desirable to choose the minimum value among each case.

#### 5.1. Prediction of remaining service life by carbonation

In the case of the well-designed and constructed structures under periodic maintenance, the remaining service life

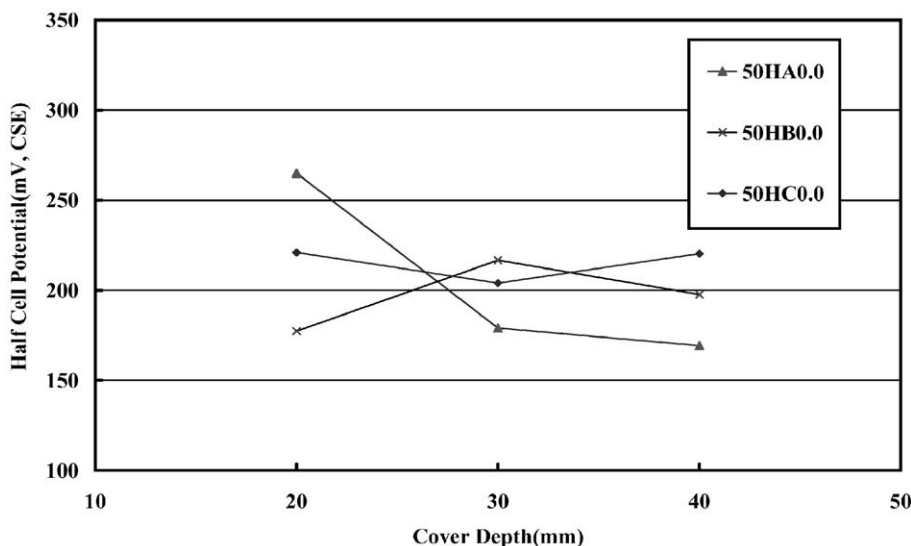


Fig. 12. Half-cell potential according to cover depth for  $w/c=0.5$ ,  $cl0.0$ .

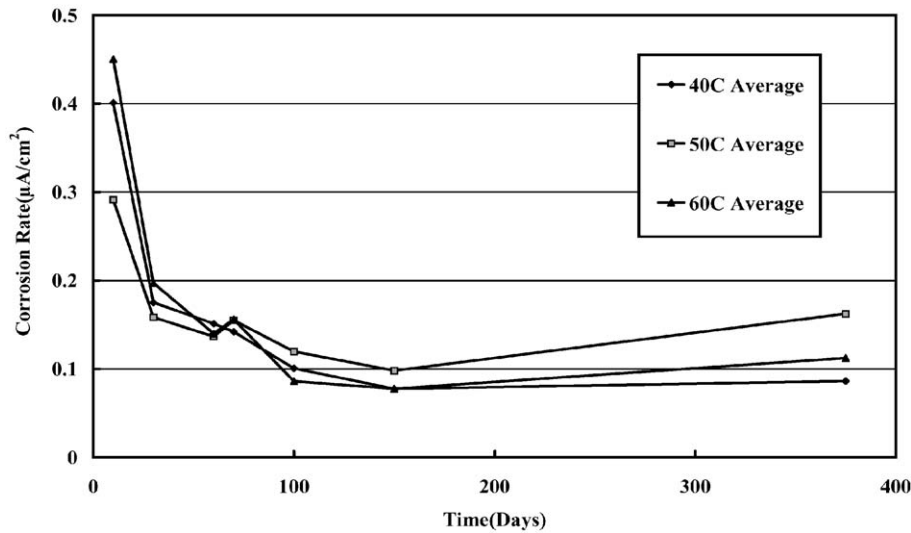


Fig. 13. Corrosion rate according to w/c and time for relative humidity 50%.

of the structures is very long if there is no deicing salts or disasters. In such conditions, the threshold time of corrosion is mainly determined by effective depth of concrete cover considering carbonation front. This paper does not consider propagation period. However, to be a more exact prediction, it need consider this period. The way to predict the service life is as follows:

1. Assume  $x = kT_{ini}^n$  as in Eq. (3).
2. After measuring the average relative humidity in the region that concrete locate, determine the  $n$  value by Eq. (4) and then calculate the yearly means of  $n$ . If the relative humidity is unknown, generally 0.5 is taken as  $n$  [18].
3. Determine the carbonation depth ( $x_1$ ) by phenolphthalein and assume depth of carbonation front ( $x_2$ ), here recommended 6mm, and then calculate effective carbonation depth ( $x$ ) by Eq. (1), and last calculate coefficient  $R$  by Eq. (3).

4. Determine the concrete cover depth  $d_1$  that is the smallest value among the cover depth of the design drawing. If it is not possible to get the deviation value of the cover depth, 8 mm is recommended on about 50 mm cover depth [9] and then determine the loss limit by corrosion ( $\alpha$ ) as intention to designer. The effective cover depth ( $d$ ) can be determined by Eq. (2).
5. Determine the initiation period ( $T_{ini}$ ) by substituting the effective cover depth  $d$  into Eq. (1).

#### 5.2. Prediction of remaining service life by sea sand

The corrosion rate measured in this experiment was expressed as the function with respect to steel loss by the

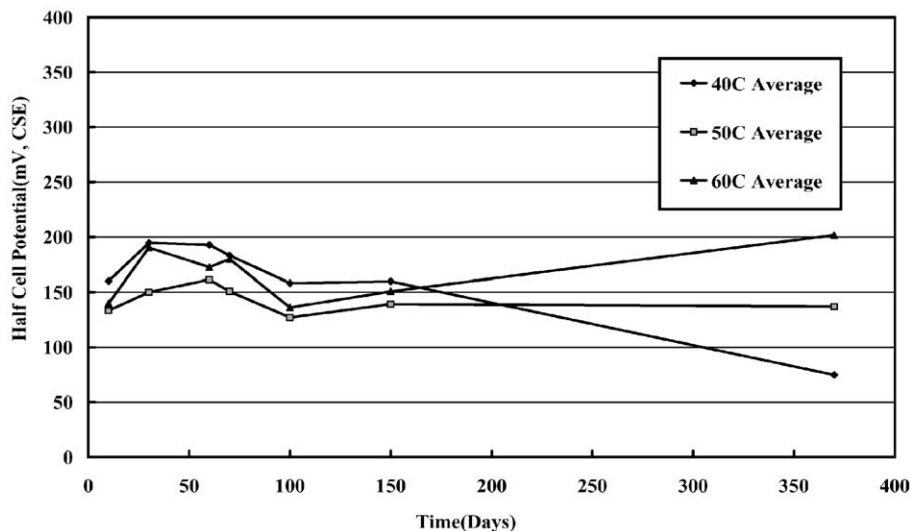


Fig. 14. Half-cell potential according to w/c and time for relative humidity 50%.

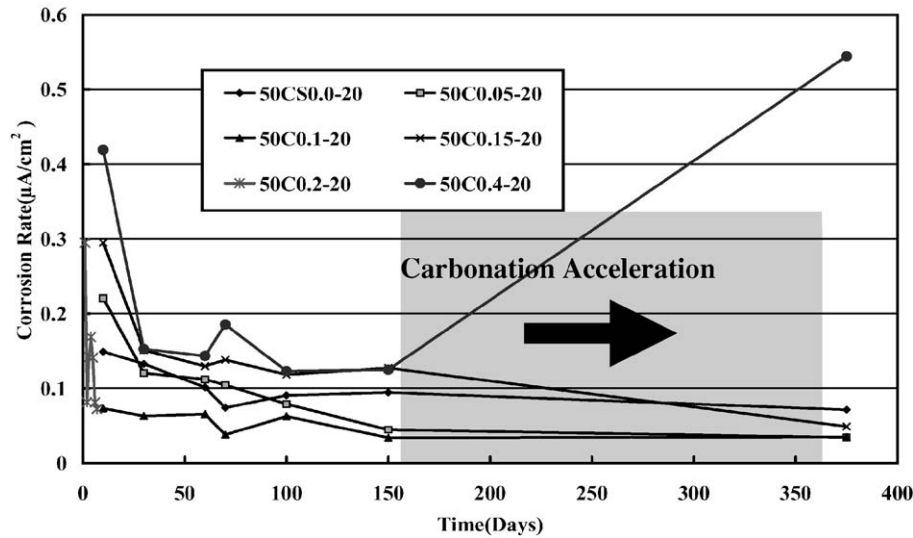


Fig. 15. Corrosion rate according to de-carbonation for  $w/c=0.5$ , cover depth 20 mm.

multiple regression analysis through the statistical analysis program, SAS. Although only three factors—the relative humidity, the chloride ion and the concrete cover depth—are considered that influence and these are available with limited ranges, it is considered as a significant function model for the corrosion using sea sand.

#### 5.2.1. Corrosion rate for relative humidity over 60%

In case that  $w/c$  was 50% and the relative humidity was over 60%, the corrosion rate was multiple regressively analyzed as an exponential function of relative humidity, chloride ion and the cover depth. Based on the SAS program, it demonstrated the appropriateness for the selected function in  $t$ -test with less than 1% significance level and also in the residual distributions. Figs. 19 and 20

show that measured data and regressive data are almost same.

$$I_{\text{corr}} = 0.01169e^{2.8899\text{Cl}-0.0120\text{De}+0.0269\text{Hu}} \mu\text{A}/\text{cm}^2 \quad (8)$$

Cl is the chloride ion contents by the weight of the cement (0–0.4%) and De is the cover depth in millimeter unit from 20 to 40 mm. Hu is the relative humidity in % from 68% to 90%.

#### 5.2.2. Corrosion rate for relative humidity under 60%

In case of data of the relative humidity under 60%, humidity factor was considered only 50% and cover depth was not considered because the significance level of the  $t$ -test statistics exceeds 40% about cover depth. Therefore,

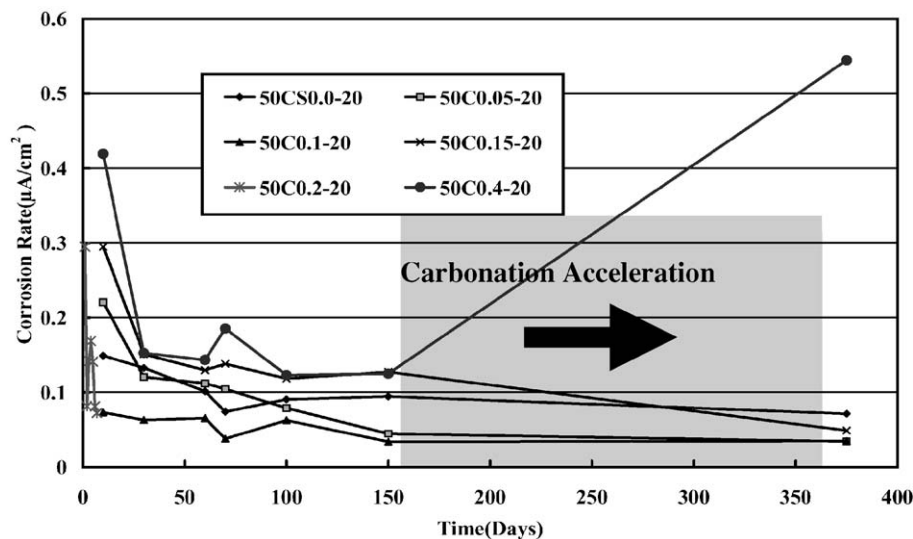


Fig. 16. Half-cell potential according to de-carbonation  $w/c=0.5$ , cover depth 20 mm.

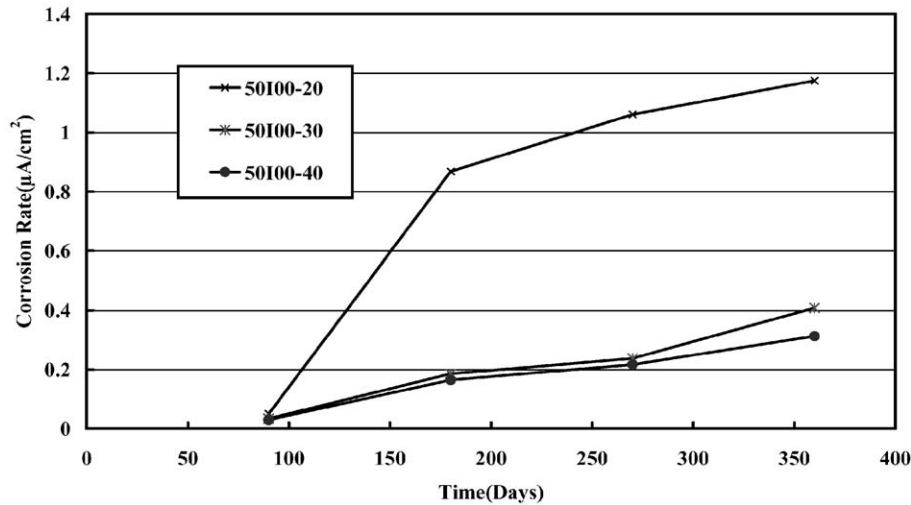


Fig. 17. Corrosion rate according to deicing use.

regressive function was performed only about the chloride ion contents. The Cl represents % weight of the cement (0–0.8%) and Fig. 21 shows the measured corrosion rates and the regressive function for the 50% relative humidity

$$I_{\text{corr}} = 0.0692e^{1.69848\text{Cl}} \mu\text{A}/\text{cm}^2 \quad (9)$$

### 5.2.3. Computation of steel loss and prediction of service life

Steel loss can be expressed by integrating the corrosion rate to the time such as Eqs. (10) and (11). And steel loss is presented as rust. When rust volume exceeds crack-induced volume, service life of concrete by corrosion is considered as the end. The rust volume to the steel loss is varied as oxidation material and the crack induced section loss, varies according to the restriction conditions such as the steel

spacing, the steel diameter and the geometric location. But this paper just deals with prediction of steel loss.

Relative humidity over 60%

$$Q_{\text{corr}} = 0.1344t \times e^{2.890\text{Cl} - 0.012\text{De} + 0.027\text{Hu}} \mu\text{m}/\text{year} \quad \text{section loss} \quad (10)$$

Relative humidity 50%

$$Q_{\text{corr}} = 0.7958t \times e^{1.699\text{Cl}} \mu\text{m}/\text{year} \quad \text{section loss} \quad (11)$$

### 5.3. Prediction of remaining service life by deicing salts

Except the case of using sea sand, if the land concrete is affected by the chloride ion, the main cause must be the

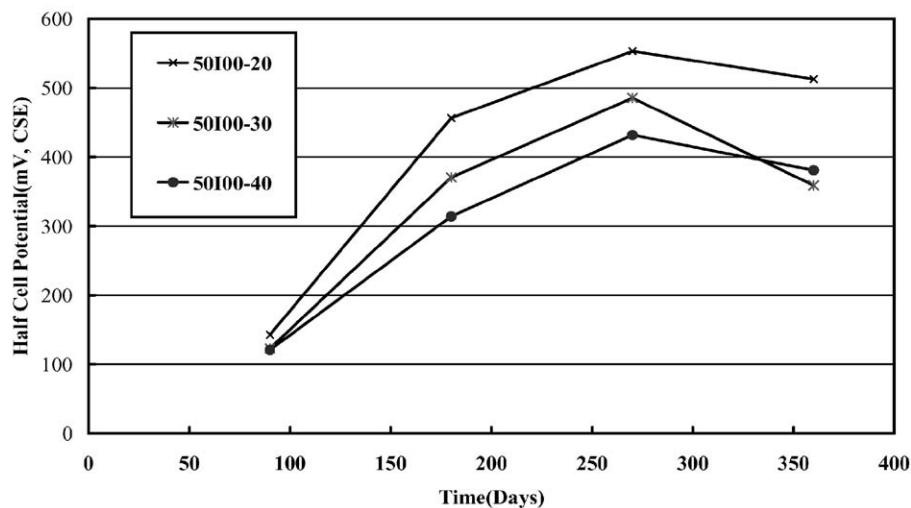


Fig. 18. Half-cell potential according to deicing use.

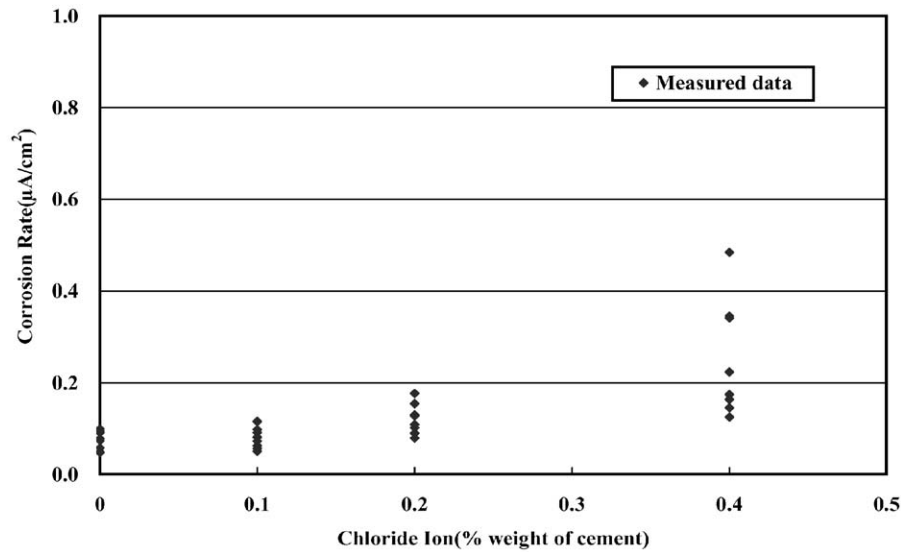


Fig. 19. Data by corrosion experiment.

usage of the deicing salts. It is, however, very difficult to generalize the effect of the deicing salts because of the irregular frequency using. Chloride contents to the time on the concrete surface is schematically assumed in Fig. 22 and it is assumed a particular function  $C(0,t)$ . The corrosion starting point is decided by the Cl/OH ratio but the standard of many countries is prescribed as the amount of Cl under the assumption that the amount of OH is not so prominently different. Eq. (12) represents the general solution of the Fick's law and by assuming the concrete surface concentration as  $C(0,t) = kt^{1/2}$ , Eq. (12) is converted as Eq. (13) [2,19]. The  $k$  constant is determined by inputting the ages and chloride ion concentrations in the concrete surface. If the Cl

amount around the steel from Eq. (13) becomes equal to the allowable value, it is predicted as the service life of the concrete.

$$C(x,t) = C_0 \left[ 1 - \operatorname{erf} \left( \frac{x}{2(D_{\text{eff}}t)^{1/2}} \right) \right] \quad (12)$$

$$C(x,t) = k\sqrt{t} \left\{ e^{-x^2/4D_{\text{eff}}T} - \left[ \frac{x\sqrt{\pi}}{2\sqrt{D_{\text{eff}}t}} \operatorname{erf} \left( \frac{x}{2\sqrt{D_{\text{eff}}t}} \right) \right] \right\} \quad (13)$$

Here, the  $C(x,t)$  means the chloride ion concentration with respect to the depth  $x$  at the age  $t$ ,  $C_0$  is the constant chloride

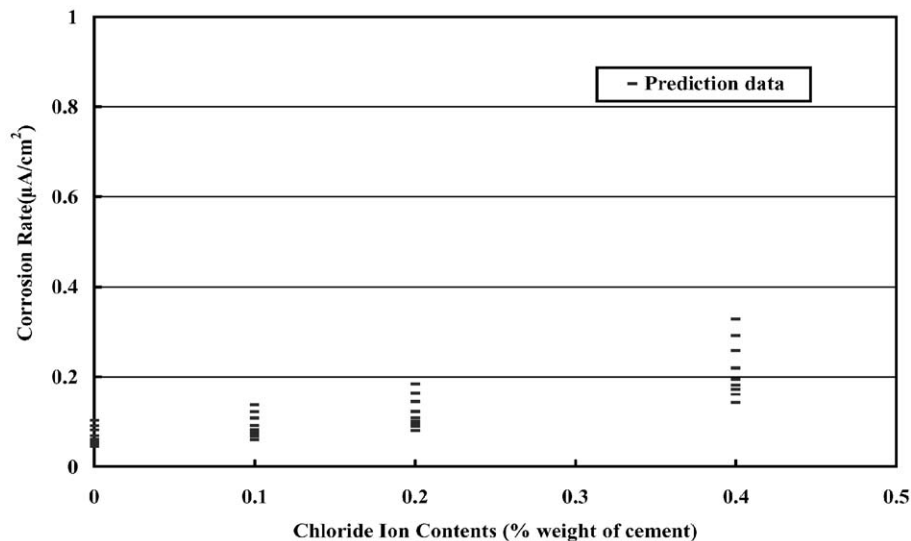


Fig. 20. Data by prediction equation.

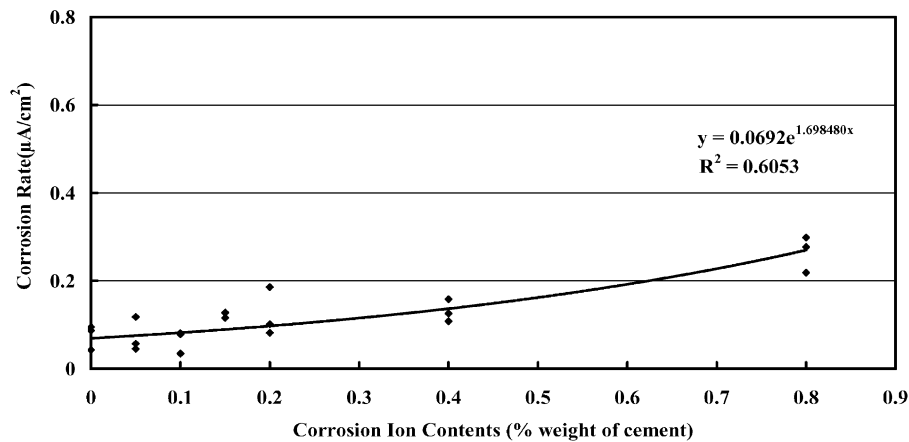


Fig. 21. Result data of corrosion test and regression graph (below relative humidity 60%).

ion concentration on the surface.  $D_{\text{eff}}$  and erf are the effective diffusion coefficient and the error function, respectively.

## 6. Conclusions

1. The quantitative polarization resistance method rather than the qualitative half-cell potential method showed more precise results in the corrosion characteristic test under the various conditions; however, it is more complex and require expensive equipments. Therefore, it is advisable to perform two methods appropriately and simultaneously in the field.
2. At the early age, the corrosion of the steel in the concrete shows unstable rate owing to the hydration process and the remaining moisture inside the concrete. Hence, in the case of analysis using the electrochemical test, it is desirable to conduct the test after 150 days.
3. The coefficient (B) that converses linear polarization resistance into corrosion rate was analyzed as 0.0438 V by measuring steel loss.

4. The pH range by the phenolphthalein indicates 8.3–9.5, but the corrosion generally occur at the range of pH 11–11.5. Furthermore, the usage of sea sand makes the threshold pH to be higher. After the investigation of five bridges, the depths of carbonation front were assessed about 3.6–8.3 mm, which implies the life-predicting gap of over 10 years.
5. Even if carbonation progressed to the bar, the corrosion rate was slow at the low relative humidity. And concrete that have much chloride ion contents developed more rapidly corrosion regardless of the other conditions.
6. The prediction equation of steel loss was derived in consideration of chloride ion contents, relative humidity and concrete cover depth.
7. The prediction of remaining service life of the land concrete by steel corrosion was suggested in three different cases of carbonation, using sea sand with the possibility of imperfect chloride elimination and using deicing salts. Although the proposed schemes have some inevitable assumptions, these are considered to be useful for assessment of the remaining service life of the land concrete.

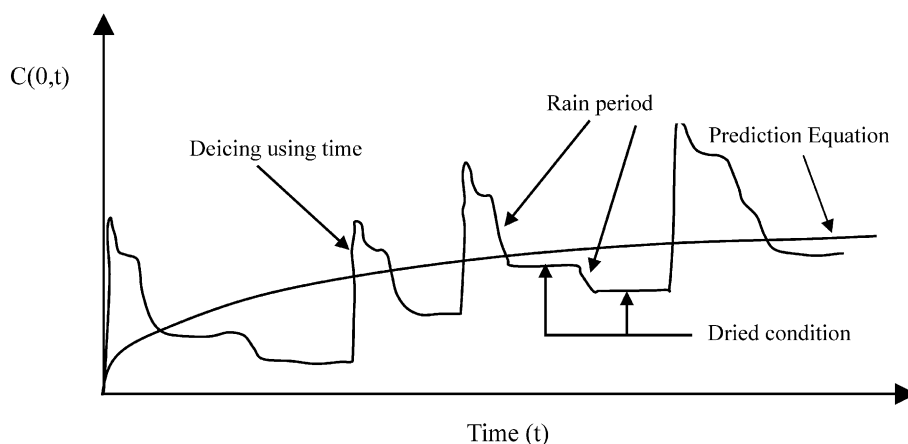


Fig. 22. Schematic description of chloride ion contents according to deicing use at concrete surface.



## Acknowledgements

The authors would like to thank the Korea Institute of Science and Technology Evaluation and Planning (KISTEP) for the financial support of National Research Laboratory (NRL).

## References

- [1] R.E. Weyers, Service life model for concrete structures in chloride laden environments, *ACI Mater. J.* 95 (4) (1988) 445–453.
- [2] S.L. Amey, D.A. Johnson, M.A. Miltenberger, H. Farzam, Predicting the service life of concrete marine structures, *ACI Struct. J.* 95 (2) (1998) 205–214.
- [3] C.Q. Li, Corrosion initiation of reinforcing steel in concrete under natural salt spray and service loading—results and analysis, *ACI Mater. J.* 97 (6) (2000) 690–697.
- [4] M. Saleem, M. Shameem, S.E. Hussain, M. Maslehuddin, Effect of moisture, chloride and sulphate contamination on the electrical resistivity of Portland cement concrete, *Constr. Build. Mater.* 10 (3) (1996) 209–214.
- [5] W.-C. Jau, D.-S. Tsay, A study of the basic engineering properties of slag cement concrete and its resistance to seawater corrosion, *Cem. Concr. Res.* 28 (10) (1998) 1363–1371.
- [6] M.N. Haque, M. Kawamura, Carbonation and chloride-induced corrosion of reinforcement in fly ash concretes, *ACI Mater. J.* 89 (1) (1992) 41–48.
- [7] P. Schiessl, Corrosion of steel in concrete, Report of the Technical Committee 60-CSC RILEM, Chapman and Hall, 1988, pp. 51–53, 56–57.
- [8] J.P. Broomfield, Corrosion of Steel in Concrete, E&FN SPON, London, UK, 1997, pp. 52–72.
- [9] R.E. Weyers, Service life estimates (SHRP-S-668), Strategic Highway Research Program, National Research Council, Washington, DC, 1993.
- [10] B.S. Diamond, N.S. Berke, Steel corrosion in concrete, E&FN SPON, 1997, pp. 48 and 158.
- [11] ASTM Standard G59-91, Standard practice for conducting potentiodynamic polarization resistance measurements, ASTM, August 15, 1991.
- [12] ASTM Standard C876-91, Standard test method for half-cell potentials of uncoated reinforcing steel in concrete, ASTM, March 11, 1991.
- [13] J. Files, Electrochemical measurements on concrete bridge for evaluation of reinforcement corrosion rates, *Corrosion*, 49 (7) (1993) 601–613.
- [14] C. Andrade, V. Castelo, C. Alonso, J.A. Gonzalez, The determination of the corrosion rate of steel embedded in concrete by the polarization resistance and AC impedance methods, Corrosion Effect of Stray Currents and the Techniques for Evaluating Corrosion of Rebars in Concrete, ASTM Spec. Tech. Publ., vol. 906, ASTM, West Conshohocken, 1986, pp. 43–63.
- [15] D.A. Jones, Principle and Prevention of Corrosion, 2nd ed., Prentice Hall, Upper Saddle River, NJ 07458, USA, 1996, pp. 158–159.
- [16] H. Yalcyn, M. Ergun, The prediction of corrosion rates of reinforcing steels in concrete, *Cem. Concr. Res.* 26 (10) (1996) 1593–1599.
- [17] J. Kropp, H.K. Hilsdorf, Performance criteria for concrete durability, RILEM Report 12, E&FN SPON, 1995, Chapters 3–4.
- [18] J.R. Clifton, Predicting the remaining service life of concrete, NISTIR 4712, National Institute of Standards and Technology, Nov. 1991, 24 pp.
- [19] Z.P. Bazant, Physical model for steel corrosion on concrete in concrete sea structure—application, *ASCE J. Struct. Div.* 105 (6) (1979) 1155–1166.
- [20] K. Tuutti, Corrosion of Steel in Concrete, Swedish Cement and Concrete Institute, Stockholm, 1982.